Connecting Microscopic L-H Transition Physics to the Power Threshold*

L. Schmitz,[1] B.A. Grierson,[2] Z. Yan,[3] P. Gohil,[4] G.R. McKee,[3] L. Zeng,[1] T.L. Rhodes,[1] J.A. Boedo,[5] D. Eldon,[2] L. Bardoczi,[1] C. Chrystal,[6] J.R. Groebner,[4] K.H. Burrell,[4] E.J. Doyle,[1] G. Wang[1]

[1]*University of California-Los Angeles, Los Angeles, CA 90095-7799, USA*
[2]*Princeton Plasma Physics Laboratory, Princeton, NJ 08543-0451, USA*
[3]*University of Wisconsin-Madison, Madison, WI 53706, USA*
[4]*General Atomics, PO Box 85608, San Diego, CA 92186-5608, USA*
[5]*University of California San Diego, La Jolla, CA 92093, USA*
[6]*Oak Ridge Associated Universities, Oak Ridge, TN 37830, USA*

A physics-based model of the L-H transition power threshold is needed to confidently extrapolate auxiliary heating requirements for burning plasmas. Two important scalings that need a physics basis are the isotope scaling, and the non-monotonic scaling of the power threshold with plasma density. The goal of this work is to link differences in the microscopic turbulence-flow interaction to the resulting macroscopic power threshold density and isotope scaling.

Evidence from several recent experiments has pointed towards a synergistic role of turbulence-driven flows [Zonal Flows (ZFs)] and pressure-gradient-driven flows in the trigger and evolution of the L-H transition [1,3-7]. L-H transitions preceded by limit cycle oscillations (LCO) between the turbulence amplitude and the $\boldsymbol{E}\times\boldsymbol{B}$ flow have been obtained in DIII-D [8,9] and other devices near the L-H power threshold P_{th}, across a large range of plasma density, current, and safety factor ($1\mathrm{x}10^{19}$ m^{-3} $\leq \langle \mathrm{n} \rangle \leq 5.5\mathrm{x}10^{19}$ m^{-3}, $0.6 \leq I_{\mathrm{p}} \leq 1.5$ MA, $3.8 \leq q_{95} \leq 8$). Detailed measurements of the $\boldsymbol{E}\times\boldsymbol{B}$ velocity and turbulence time evolution across the L-LCO-H-mode transition have been reported previously [8,9]. Here we present direct evidence that the $\boldsymbol{E}\times\boldsymbol{B}$ velocity modulation at the start of the LCO phase (t_{LCO}) is dominated by the ion poloidal velocity [Fig.1(a)] that is driven via the perpendicular Reynolds stress [Fig.1(b)]. We use a phase-lock analysis technique to improve the signal-to-noise ratio of the main ion CER data and extract an estimate of the time-resolved poloidal ion flow velocity modulation. The $\boldsymbol{E}\times\boldsymbol{B}$ velocity is measured via Doppler Backscattering [10,11]. Fig.1(a) shows that the measured poloidal ion flow modulation accounts within error margins for the measured flow modulation (the offset is due to L-mode diamagnetic flow and toroidal flow related to NBI co-injection). No modulation of the ion pressure gradient ∇P_i is found initially during the LCO phase [1,9] or during the initial trigger phase of regular fast L-H transitions [8,12], but it has been shown previously that the pressure gradient dominates the $\boldsymbol{E}\times\boldsymbol{B}$ shear ultimately later in the LCO phase, locking in the H-mode transport barrier. The modulation of the toroidal flow velocity (not shown here) is a small fraction of the mean parallel velocity resulting from the co-NBI beam torque, and is out-of-phase with the poloidal velocity.

The poloidal ion flow acceleration via the Reynolds stress $<\tilde{v}_r\tilde{v}_\theta>$ can be expressed as $(1+2q^2)\partial<v_{i\theta}>/\partial t = -\partial<\tilde{v}_r\tilde{v}_\theta>/\partial r - \mu<v_{i\theta}>$ [13], where μ is the flow damping rate towards the neoclassical flow.

Fig. 1(b) shows a comparison of the measured flow acceleration with the Reynolds stress gradient evaluated via BES (Beam Emission Spectroscopy) velocimetry. The poloidal flow damping (in the plateau regime) is expected to be small here compared to the first two terms in the above equation, and is not evaluated. It is clear from Fig.1(b) that the Reynolds stress radial gradient is sufficiently large across the edge layer to account for the observed (dipolar) poloidal flow acceleration during the early LCO phase.

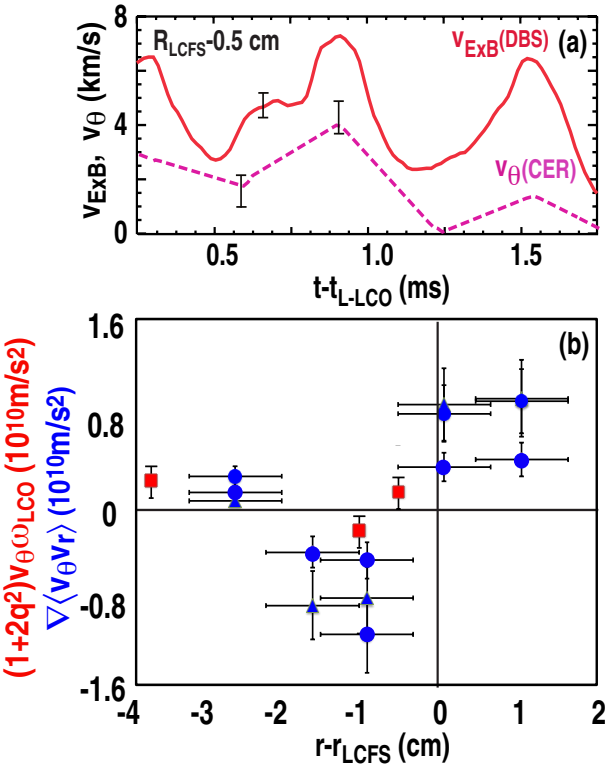

Fig.1: (a) Time evolution ExB velocity and poloidal main ion velocity during the initial LCO cycles; (b) Measured poloidal flow acceleration compared to Reynolds stress radial gradient (r_{LCFS} is the separatrix radius).

The energy transfer from the ambient L-mode turbulence into directional meso-scale flows is an important quantity that couples the L-H trigger dynamics to the power threshold scaling. This energy transfer has been described by a rate equation for the (low frequency) flow energy W (where $<\tilde{v}_\theta\tilde{v}_r>$ is the Reynolds stress and v_θ is the poloidal ion flow [14]):

$$\frac{\partial W}{\partial t} = <\tilde{v}_\theta\tilde{v}_r>\frac{\partial v_\theta}{\partial r} - \gamma_{ZF}W - \frac{\partial}{\partial r}<\tilde{v}_\theta\tilde{v}_r>v_\theta \qquad (1)$$

Neglecting the Zonal flow damping rate γ_{ZF} and the fourth term describing radial energy spreading, the energy transfer rate is proportional to the (L-mode) seed flow shear $\partial v_\theta/\partial r$ and to the Reynolds stress. The measured maximum $\boldsymbol{E}\times\boldsymbol{B}$ and $\mathbf{v}\times\boldsymbol{B}$ flow shearing rates ~0.5 cm inside the LCFS (the latter quantity evaluated from $\omega_{\mathbf{E}\times\mathbf{B}}$ via subtracting the measured diamagnetic shear) are shown in Figure 2(a), for deuterium (D) and hydrogen (H) plasmas, in lower single null ITER-similar (ISS) shape. Both the (total) $\boldsymbol{E}\times\boldsymbol{B}$ shearing rate and the $\mathbf{v}\times\boldsymbol{B}$ flow shearing rate in equation (1) increase towards low and high plasma density, and are smaller near the power threshold minimum [Fig.2(c), $<n>_{min}$~2-3x10^{19} m^{-3}]. The diamagnetic shear [shown in Fig. 2(b)] increases also at low density, and is larger in deuterium plasmas. Figure 2(c) shows the power threshold (loss power across the separatrix)

for D and H "regular" fast L-H transitions in the ISS shape as well as LCO transitions (D) with a lower x-point height and correspondingly reduced power threshold [15].

From Fig. 2 we can conclude that (i) the L-mode $\boldsymbol{E}\times\boldsymbol{B}$ shear depends on density and peaks at low density; (ii) the L-mode seed flow shear is small near $\langle n\rangle_{min}$ but is significant at low and high density, and therefore scales similarly with density as the L-H transition power threshold; (iii) the L-mode diamagnetic flow shear, and the seed flow shear just before the transition is higher in D than in H, particularly in the low density branch of the power threshold, and may facilitate the L-H transition in D as observed in the power threshold isotope scaling.

Fig.3(a) shows that the increased diamagnetic shear in the D-plasma is primarily due to a lower L-mode edge density gradient. Very little difference was found in the ion temperature gradient (not shown here). Fig. 3(b) shows that the $\boldsymbol{E}\times\boldsymbol{B}$ velocity inside the last closed flux surface has a less pronounced well structure in H-plasmas compared to D-plasmas, and that the velocity shear in the outer and in the inner flow shear layer is reduced. Fig. 3(c) shows that density fluctuations levels (at $k_a\rho_s\sim0.5$) are higher in the H-plasma, consistent with either higher instability growth rates or lower $\boldsymbol{E}\times\boldsymbol{B}$ shear (as observed here), However, larger scale density fluctuations measured by BES show the opposite behavior in H and D.

We have presented evidence that turbulence-driven poloidal ion flow is the dominant contribution to the $\boldsymbol{E}\times\boldsymbol{B}$ velocity modulation early during the LCO phase. As such it is responsible for the initial turbulence suppression during the LCO

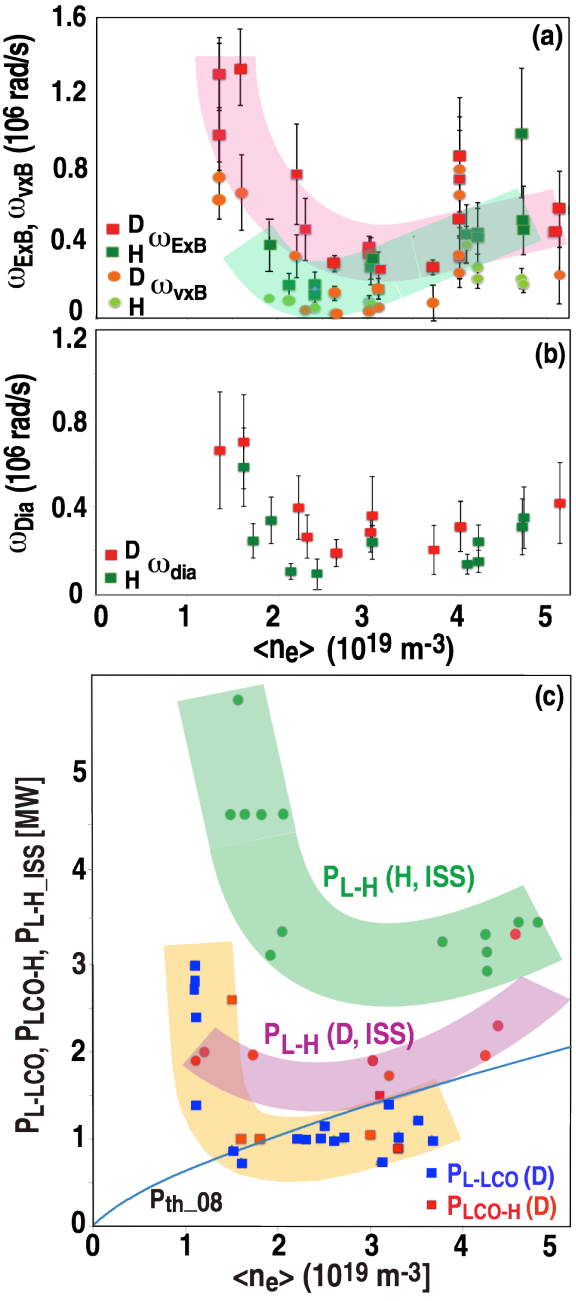

Fig.2: (a) L-mode $\boldsymbol{E}\times\boldsymbol{B}$ flow shearing rate and $\boldsymbol{v}\times\boldsymbol{B}$ component vs density; (b) L-mode diamagnetic flow shear in D and H ISS plasmas; (c) measured power threshold for L-mode-LCO and LCO-H-mode transitions (D) and L-H transitions in ISS-shape (D and H) compared to the 2008 empirical (Martin) scaling (P_{th_08} [3]).

phase, as demonstrated earlier [9]. It is also shown here that the L-mode seed flow shear increases in particular in the low density branch of the power threshold [Fig.2(a)], and that the L-mode ***E×B*** shear and diamagnetic shear increase with decreasing line averaged density below n_{min}, the density where the power threshold is lowest, and depend on ion species [Fig.2(a,b)]. This result is in contrast to previous reports where no density dependence of the L-mode ***E×B*** flow shear was observed [16,17]. Accordingly, the turbulence-flow energy transfer rate may increase with the threshold power in the low- and high-density branches of the power threshold scaling. Further work is needed to clarify whether this effect contributes to, or explains, the non-monotonic dependence of the L-H transition power threshold on plasma density.

*This work was supported by the U.S. DOE under DE-FG03-01ER54615, DE-AC02-09CH11466, DE-FG02-89ER53296, DE-FG02-08ER54999, DE-FG02-07ER54917 and DE-FG02-08ER54984.

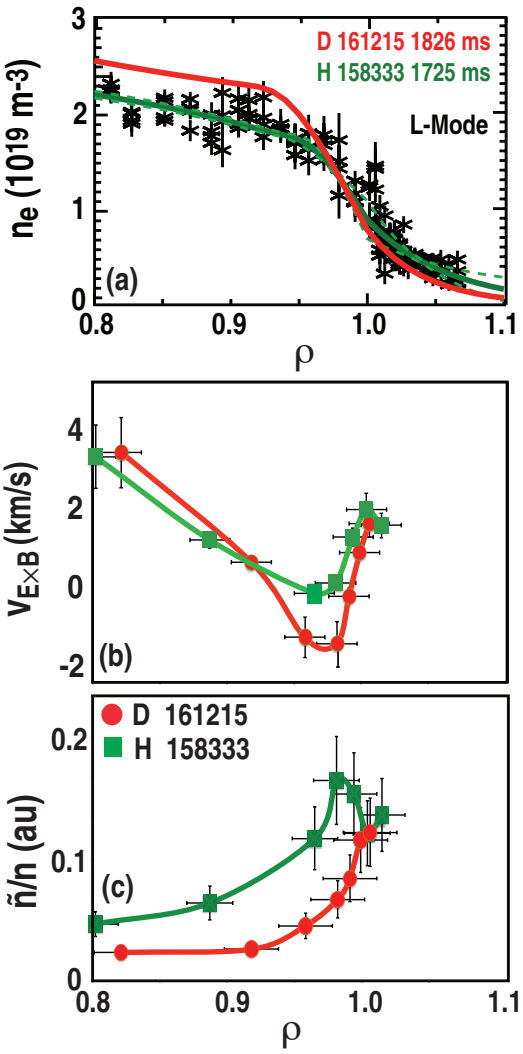

*Fig.3: (a) Plasma density, (b) **E×B** velocity profile, and (c) normalized DBS density fluctuation level in D- and H-plasmas (<n>=3x10^{19} m^{-3}). Loss power past LCFS is within 1 MW above P_{th}.*

[1] L. Schmitz, L. Zeng, T.L. Rhodes, et al., Phys. Rev. Lett. **108**, 155002-5 (2012).
[2] K. Miki and P.H. Diamond, Phys. Plasmas **19**, 092306 (2012).
[3] G.R. McKee et al., Nucl. Fusion **49**, 115016 (2009).
[4] S.J. Zweben, R.J.Maqueda, R. Hager, et al., Phys. Plasmas **17**, 102502 (2010).
[5] G.D. Conway, C. Angioni, F. Ryter, et al., Phys. Rev. Lett. **106**, 065001 (2011).
[6] G.S. Xu et al., Phys. Rev. Lett. **107**, 125001 (2011).
[7] T. Estrada, C. Hidalgo, T. Happel, et al., Phys. Rev. Lett. **107**, 245004 (2011).
[8] L. Schmitz et al., Nucl. Fusion **54** 073012 (2014).
[9] L. Schmitz et al., Paper EX/11-4, 25th IAEA Fusion Energy Conference, October 13-18, 2014, St. Petersburg, Russian Federation
[10] W.A.Peebles, T.L. Rhodes, J.C. Hillesheim, et al., Rev. Sci. Instrum. **81**, 10D902 (2010).
[11] J.C. Hillesheim et al., Rev. Sci. Instrum. **81**, 10D907 (2010).
[12] I. Cziegler, G.R. Tynan, P.H. Diamond, et al., Plasma Phys. Control. Fusion **56** 075013 (2014).
[13] P.H. Diamond, and Y.-B. Kim, Phys. Fluids **B3**, 1626 (1991)
[14] G. Tynan, et al. Nucl. Fusion **53,** 073053 (2012).
[15] P. Gohil, et al., Nucl. Fusion **51**,103020 (2011).
[16] P. Sauter, C. Puetterich, F. Ryter, et al., Nucl. Fusion **52**, 012001 (2012).
[17] C. Maggi, E. Dalabie, T.M. Biewer, et al. Nucl. Fusion **54** 023007 (2014)